DFB Lasers With Deeply Etched Vertical Grating Based on InAs–InP Quantum-Dash Structures

Klaus Mathwig, Wolfgang Kaiser, André Somers, Johann Peter Reithmaier, *Member, IEEE*, Alfred Forchel, *Associate Member, IEEE*, Kazuya Ohira, *Student Member, IEEE*, Saeed M. Ullah, and Shigehisa Arai, *Member, IEEE*

***Abstract*—Distributed feedback lasers with first-order vertical grating based on AlInGaAs–InAs–InP quantum-dash lasers were fabricated by electron beam lithography and Cl_2–Ar reactive ion etching with an electron cyclotron resonance source. Low threshold currents and single-mode operation with sidemode suppression ratios of 48 dB and a direct modulation bandwidth of 5.5 GHz were demonstrated.**

***Index Terms*—Deep etching, distributed feedback (DFB) laser, quantum dot, vertical grating.**

I. Introduction

SEMICONDUCTOR lasers with stable single-mode operation are crucial devices for optoelectronic communication systems. For fiber-optics applications near wavelengths of 1.55-μm, quantum dashes (QDash) grown on InP were developed as a low-dimensional optical gain material [1]–[3]. Single-mode InP QDash lasers are reported in this letter. We describe the fabrication of QDash distributed feedback (DFB) lasers in addition to their basic static and dynamic properties. Since their first demonstration by Miller *et al.* [4], ridge waveguide lasers with vertical etched gratings experienced a rapid development [5], [6] for devices based on quantum-well structures. In our work, first-order gratings are used instead of the original third- and fifth-order gratings and the ridge waveguide is shrunk down to a width of only 2 μm. Since the diffraction grating and mesa structure are fabricated simultaneously, only few processing steps are necessary. To achieve a sufficient coupling, the grating and mesa structure were deeply etched below the active layer by Cl_2–Ar reactive ion etching with an electron cyclotron resonance (ECR) source. The more commonly used method to process this kind of laser design by repeated cycles of CH_4–H_2 reactive ion etching and O_2 ashing [7] could not be applied due to the high aluminum content of quaternary waveguiding and cladding layers which are removed with a negligibly slow rate. Thus, we developed a new etching process and a technique to pattern a SiO_2 etching mask with high resolution.

Manuscript received September 12, 2006; revised December 17, 2006. This work was supported by the State of Bavaria.

K. Mathwig was with Technische Physik, Universität Würzburg, 97074 Würzburg, Germany. He is now with Max Planck Institute of Microstructure Physics, 06120 Halle, Germany (e-mail: kmathwig@mpi-halle.mpg.de).

W. Kaiser, A. Somers, and A. Forchel are with Technische Physik, Universität Würzburg, 97074 Würzburg, Germany.

J. P. Reithmaier was with Technische Physik, Universität Würzburg, 97074 Würzburg, Germany. He is now with the Institute for Nanostructure Technologies and Analytics, Technische Physik, Universität Kassel, 34132 Kassel, Germany.

K. Ohira, S. M. Ullah, and S. Arai are with the Quantum Nanoelectronics Research Center, Tokyo Institute of Technology, Tokyo 152-8552, Japan.

Digital Object Identifier 10.1109/LPT.2007.891206

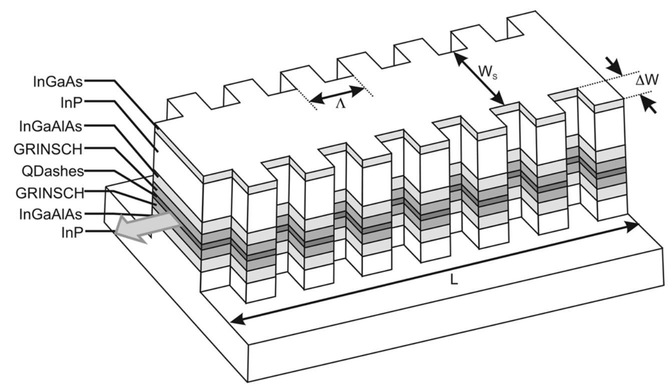

Fig. 1. Schematic structure of a VG-DFB laser.

The fabricated DFB lasers exhibit threshold currents as low as 24 mA, room-temperature continuous-wave (CW) operation up to 55 °C, a large 48-dB sidemode suppression ratio (SMSR), and a modulation bandwidth under CW bias of 5.5 GHz.

II. Fabrication

The active region consists of four InAs QDash layers separated by 10-nm-thick AlInGaAs barriers. The layers were grown by solid state epitaxy with the InAs dash layer having a nominal deposition depth of four monolayers. The active region is sandwiched in between 100-nm-thick AlInGaAs GRINSCH layers surrounded by 80-nm-thick AlInGaAs cladding layers. The upper cladding consists of a 1760-nm-thick p-doped InP layer, covered by a highly doped 150-nm-thick InGaAs contact layer. All layers, except the QDash layers, are lattice-matched to InP.

Fig. 1 shows a schematic structure of a deeply etched vertical-grating (VG)-DFB laser. Devices with stripe widths (W_S) of 2 and 3 μm and lateral grating widths (ΔW) between 150 and 400 nm were fabricated. The grating period (Λ) ranges from 230 to 240 nm for first-order gratings and 460 to 480 nm for second-order gratings (mark-space ratio approximately 1 : 2), respectively.

A 200-nm-thick SiO_2 layer was deposited on the sample as mask material for the Cl_2–Ar ECR-RIE dry-etching process. Polymethylmethacrylate (PMMA) was spin-coated and vertical grating and mesa stripe patterns were drawn simultaneously by high-resolution electron beam lithography.

In contrast to the fabrication of, e.g., photonic crystals (PCs) where the SiO_2 is patterned directly by using PMMA as mask material, a different approach has to be taken for the VG-DFB

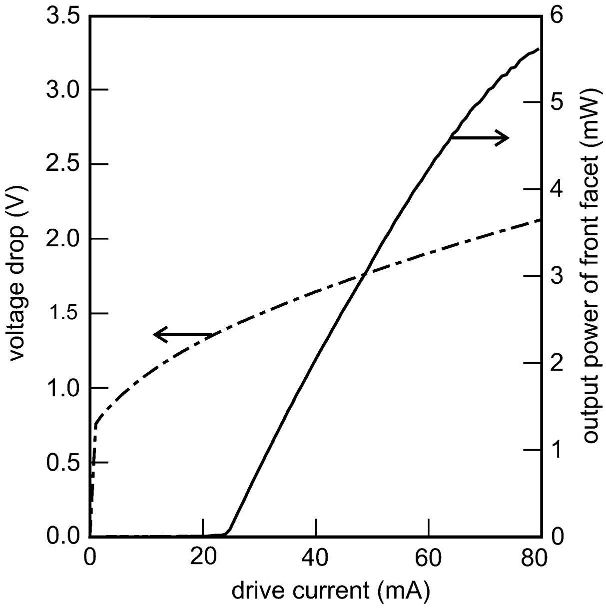

Fig. 2. P–I and voltage–current curve of a 0.5-mm-long and 2-μm-wide VG-DFB laser with back-facet HR-coated. The laser is operated in CW mode at room temperature.

lasers. In the PC case, the exposed areas are etched, so patterning of SiO_2 would either be possible with negative resist or by exposing the inverse structure while still using PMMA. Instead, titanium was evaporated and selectively removed by the standard liftoff technique to form a mask for dry-etching the SiO_2 layer. The pattern was transferred to the SiO_2 by 30 min of CHF_3–Ar reactive ion etching. The Ti was removed almost entirely during this process. Compared to the 500-nm-thick PMMA in the PC-case [8], only a thin 100-nm-thick Ti mask is necessary. For a successful liftoff process, 150 nm of PMMA are sufficient. Therefore, a higher resolution of the SiO_2 pattern and also of the deeply etched semiconductor is achieved.

The whole structure was etched below the active region. After 420 s of Cl_2–Ar ECR etching (0.8 Pa, 6% Cl_2 fraction of 20-sccm flow rate, 125-W RF power, 1000-W ECR power) a mesa height of about 3 μm was obtained. The remaining SiO_2 mask material was removed by 180 s of CHF_3–Ar etching to open up the contact layer again. The sample was planarized by bisbenzocyclobutene before the p- and n-contact layers were evaporated. The devices were cleaved and for some lasers one facet was high-reflection (HR)-coated.

III. Device Characterization

Fig. 2 shows the light–output characteristics of a 0.5-mm-long and 2-μm-wide VG-DFB laser with a lateral grating width ΔW of 150 nm. The device is unmounted and operated in CW mode. The light was detected from the as-cleaved facet, which corresponds to 75% of the total output power. At room temperature, a low threshold current of only 24 mA, a slope efficiency as high as 0.12 W/A, and a maximum output power from the front facet of 5.5 mW were achieved, which is comparable to the properties of laterally coupled DFB lasers with chromium-based gratings [1]. This laser has a first-order grating period of 236 nm and emits single-mode at a wavelength of 1517 nm with an SMSR of 28 dB at 35-mA drive current.

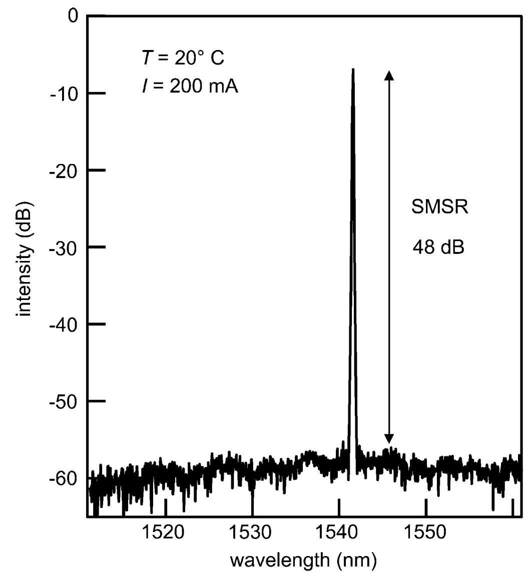

Fig. 3. Emission spectrum of a 2-mm-long DFB laser at 20 °C with CW drive current of 200 mA.

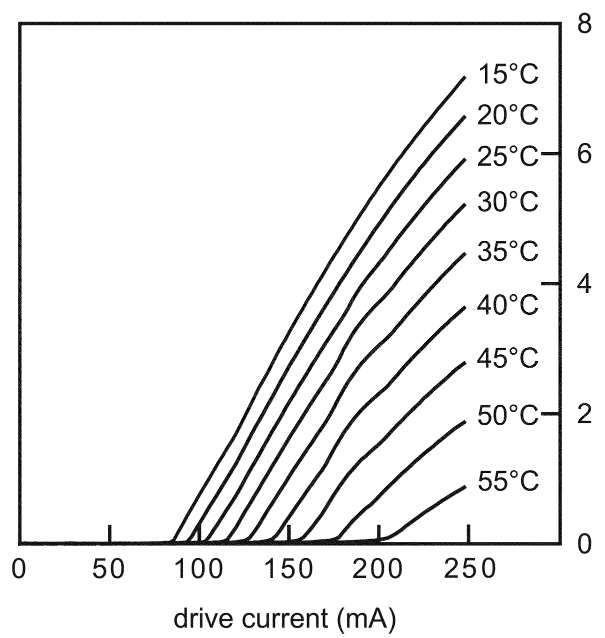

Fig. 4. P–I curves of a 2-mm-long VG-DFB laser at different CW operation temperatures. The device is as-cleaved.

Fig. 3 shows the emission spectrum of a 2-mm-long device with a second-order grating ($W_S = 2\,\mu$m, $\Delta W = 300\,\mu$m, $\Lambda =$ 480 nm, as-cleaved). At a CW bias of 200 mA, the laser emits with a high 48-dB SMSR at 1542 nm. However, the coupling strength is too weak to see a clear indication for a stopband in subthreshold spectra. The laser was measured under CW operation at different temperatures. The light–current (P–I) curves are shown in Fig. 4. Up to a temperature of 55 °C, output powers of more than 1 mW were achieved. For all devices, the temperature coefficient for the wavelength shift was measured to be 0.10 nm/K, consistent with previously reported values for DFB and DBR lasers based on QDash media [9]. The main results for lasers with different parameter sets are summarized in Table I. In general, at the current stage of development VG-DFB

TABLE I
THRESHOLD CURRENT, EFFICIENCY, AND SMSR FOR DEVICES WITH DIFFERENT GEOMETRIES AND GRATING PARAMETERS

length (μm)	500	500	800	800	800	2000	2000
W_S (μm)	2	3	2	2	4	2	3
W (nm)	150	300	150	300	400	300	300
grating order	1^{st}	2^{nd}	1^{st}	1^{st}	2^{nd}	2^{nd}	2^{nd}
HR-coating	X	X	–	–	–	–	–
threshold current (mA)	24	25	37	41	69	93	91
efficiency (W/A)	0.12	0.15	0.09	0.09	0.12	0.03	0.05
SMSR (dB)	28	34	28	21	23	48	29

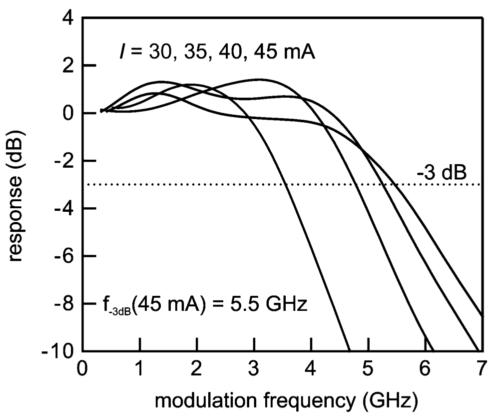

Fig. 5. Small-signal response of a 0.5-mm-long laser at four different CW bias levels.

lasers show lower SMSR values for shorter devices than their chromium counterparts [1]; only longer devices can compete with those. There is still room for improvements by optimizing the device geometry, the mark-space ratio, and the parameters of the ECR etching process.

For modulation bandwidth measurements, the lasers were mounted epi-side up on a high-frequency test fixture to insure a good electrical and thermal contact. The measurements were performed with a Hewlett Packard optical network analyzer. Under CW operation, the -3-dB bandwidth of a laser with the same geometry as the 0.5-mm-long device discussed above was measured. The resonance frequency increases from 2 GHz at a drive current of 30 mA to its maximum of about 4.5 GHz at 45 mA. This results in a -3-dB frequency of 5.5 GHz. Fig. 5 shows that for higher currents, the response is limited by a high damping which is characteristic for QDash structures [1], [9].

IV. CONCLUSION

We have reported on the fabrication and performance of VG-DFB lasers based on InP QDash gain media operating in the fiber-optics wavelength range near 1.55 μm. Mesa stripes and vertical gratings were simultaneously fabricated by Cl_2–Ar ECR etching technique. We have demonstrated a low threshold current of 24 mA, CW operation up to 55 °C, a 48-dB SMSR, and a modulation bandwidth of 5.5 GHz.

ACKNOWLEDGMENT

The authors would like to thank M. Emmerling and A. Wolf for technical assistance in device processing.

REFERENCES

[1] J. P. Reithmaier *et al.*, "InP based lasers and optical amplifiers with wire-dot-like active regions," *J. Phys. D: Appl. Phys.*, vol. 38, pp. 2088–2102, Jun. 2005.
[2] S. Deubert, A. Somers, W. Kaiser, R. Schwertberger, J. P. Reithmaier, and A. Forchel, "InP-based quantum dash lasers for wide gain bandwidth applications," *J. Cryst. Growth*, vol. 278, pp. 346–350, May 2005.
[3] R. H. Wang, A. Stintz, P. M. Varangis, T. C. Newell, H. Li, K. J. Malloy, and L. F. Lester, "Room-temperature operation of InAs quantum-dash lasers on InP (001)," *IEEE Photon. Technol. Lett.*, vol. 13, no. 8, pp. 767–769, Aug. 2001.
[4] L. M. Miller, J. T. Verdeyen, J. J. Coleman, R. P. Bryan, J. J. Alwan, K. J. Beernink, J. S. Hughes, and T. M. Cockerill, "A distributed feedback ridge waveguide quantum well heterostructure laser," *IEEE Photon. Technol. Lett.*, vol. 3, no. 1, pp. 6–8, Jan. 1991.
[5] J. Wiedmann, K. Ebihara, H.-C. Kim, B. Chen, M. Ohta, K. Matsui, S. Tamura, J.-I. Shim, and S. Arai, "1.5 μm wavelength distributed reflector lasers with vertical grating," *Electron. Lett.*, vol. 37, no. 13, pp. 831–832, Jun. 2001.
[6] H.-C. Kim, H. Kanjo, T. Hasegawa, S. Tamura, and S. Arai, "1.5 μm-wavelength narrow stripe distributed reflector lasers for high-performance operation," *IEEE J. Sel. Topics Quantum Electron.*, vol. 9, no. 5, pp. 1146–1152, Sep./Oct. 2003.
[7] M. M. Raj, S. Toyoshima, and S. Arai, "Multiple micro-cavity laser with benzocyclobutene/semiconductor high reflective mirrors fabricated by CH_4/H_2-reactive ion etching," *Jpn. J. Appl. Phys.*, vol. 38, no. 7B, pt. 2, pp. L 811–L 814, Jul. 1999.
[8] H. Scherer, D. Gollub, M. Kamp, and A. Forchel, "Tunable GaInNAs lasers with photonic crystal mirrors," *IEEE Photon. Technol. Lett.*, vol. 17, no. 11, pp. 2247–2249, Nov. 2005.
[9] W. Kaiser *et al.*, "Static and dynamic properties of laterally coupled DFB lasers based on InAs/InP QDash structures," *Electron. Lett.*, vol. 41, no. 14, pp. 808–810, Apr. 2005.